An Automatic Fault Detection and Localization Strategy for Switched Reluctance Machine Open-Circuit Fault in EVs Applications

Yakoub Saadi, Rabia Sehab, Ahmed Chaibet, Mousaa Boukhnifer, Demba Diallo

An Automatic Fault Detection and Localization Strategy for Switched Reluctance Machine Open-Circuit Fault in EVs Applications

Conference Paper · July 2019

DOI: 10.1109/ICCAD46983.2019.9037933

5 authors, including:

Saadi Yakoub
National Institute of Applied Science
9 PUBLICATIONS **41** CITATIONS
SEE PROFILE

Rabia Sehab
Ecole Supérieure des Techniques Aéronautiques et de Construction Automobile
34 PUBLICATIONS **178** CITATIONS
SEE PROFILE

Ahmed Chaibet
Institut Supérieur de l'Automobile et des Transports
92 PUBLICATIONS **572** CITATIONS
SEE PROFILE

Moussa Boukhnifer
University of Lorraine
164 PUBLICATIONS **1,420** CITATIONS
SEE PROFILE

An Automatic Fault Detection and Localization Strategy for Switched Reluctance Machine Open-Circuit Fault in EVs Applications

Yakoub SAADI
ESTACA Engineering School
Laval, France
yakoub.saadi@estaca.fr

Rabia SEHAB
ESTACA Engineering School
Laval, France
rabia.sehab@estaca.fr

Ahmed CHAIBET
ESTACA Engineering School
Paris, France
ahmed.chaibet@estaca.fr

Mousaa BOUKHNIFER
ESTACA Engineering School
Paris, France
moussa.boukhnifer@estaca.fr

Demba DIALLO
Group of Electrical Engineering - Paris (GeePs)
Paris, France
demba.diallo@geeps.centralesupelec.fr

***Abstract*—In recent years, urban electric vehicles have experienced significant growth in acquisition on the automotive market. Because of this growth and their use, these vehicles would be exposed to faults during driving causing emergency stops. A maintenance intervention is necessary to identify these faults. Among the faults that can occur on the vehicle, we are particularly interested in the electrical faults. The objective of this paper is to detect and locate automatically the open circuit faults of the electronic power converter associated to four phases 8/6 Switched Reluctance Machine used in an electric vehicle drivetrain. The developed methodology is based on spectral analysis using the FFT algorithm with a periodic sliding window for total reference torque provided by the velocity controller and measured current of each phase. Finally, the development methodology is validated on the simulator of the electric vehicle drivetrain creating an open circuit fault in any phase of the converter / Switched Reluctance Machine with a vehicle load torque. Moreover, this methodology could be extended to detect more than one open circuit fault. However, this strategy could be beneficial to implement it in the control unit of electric vehicles to identify and to locate an open circuit fault automatically. Finally, the development methodology is validated on the simulator of the electric vehicle drivetrain creating an open circuit fault in any phase of the converter / Switched Reluctance Machine with a vehicle load torque.**

***Index Terms*—Electric Vehicle, Switched Reluctance Machine, Power Conveter, Open circuit, Fault-Detection, Fault-Localization, Spectral Analysis, FFT Algorithm.**

I. Introduction

NOWADAYS automotive industrials have taken a real ecological conscience and responsibilities because of the environmental pollution due to conventional vehicles. However, hybrid and electric vehicles have seen a new demand in the automotive market, particularly the electric vehicles which are becoming the future of green transport. Also, significant development is undergoing by worldwide manufacturers to provide different technologies for electric vehicles (EVs) using mainly induction and permanent magnet machines. Today, many efforts have been devoted to developing a rare-earth-free or rare-earth-less machine for future EVs to replace the current electric machine with permanent magnets made from rare-earth materials such as neodymium, iron, boron, cobalt, and samarium. These efforts are due to the rare-earth materials which become costly with an eventual risk of supply disruption [1]. Switched Reluctance Machine (SRM), which do not use permanent magnets, is today a mature technology shows great promise as a replacement technology for electric propulsion applications [2].

The SRM is a doubly salient machine with phase coils mounted around diametrically opposite stator poles. The rotor is a piece of steel, and its shape forms salient poles with no windings or permanent magnets. Furthermore, to its simple construction that makes it inexpensive, the SRM has several advantages which allow it, not only to be a potential candidate but, to concurrence the traditional machines namely its high performance in a large wide torque/velocity range, its high reliability, its fault-tolerance operating capability and the simplicity of its power converter. Despite its advantages, it also has drawbacks such as high ripple torque and acoustic noises [3]. Nevertheless, these disadvantages can be considerably reduced with an optimal mechanical design [4] and a suitable control strategy [5].

In literature, prime focus has been given to improving efficiency, robust control, torque ripple minimization and sensorless control of SRM [6], while reliability and diagnosis research have not attracted much attention. In such an application, if a fault has occurred, it primordial to provide an integrated fault-detection followed by fault tolerant strategies to ensure the operating of the EV until maintenance can be performed.

In general, the detection and localization of faults required the knowledge of the healthy behaviors of the system to compare it with the symptoms characteristic in the failure mode and

978-1-7281-2292-2/19/$31.00 ©2019 IEEE

their analysis to deduce the state of the system.
Several failures can affect the Switched Reluctance Machines, systematic classification of all electrical faults, for short and open circuits in the SRM drive is given in [7]. In contrast, many detections and localization techniques have been proposed in SRM. The electrical fault-detection methods can be regrouped in two classes: the first based on hardware detectors and the second on software algorithms.
A comparison of several hardware-based fault detection methods is presented in [8], such as an overcurrent detector, a current differential detector and a flux differential detector. The detectors based on current sensors are easy to implement but not fast acting since a fault indication is not set until the current is already very high. The fault-detectors using magnetic field sensors are fast acting, but their implementation is complicated and required induction coil (search coil), which cannot be placed on an existing commercial SRMs. Also, the sensors are subject to damage and the distinguish between sensor faults and electrical faults of the machine cannot be achieved in this fault-detection methods.
Different algorithms are used for electrical fault-detection, Artificial Intelligence (AI)-based method is used in [9] for diagnosing and tracking the short phase faults in SRM. The purpose of this technique is to classify the data obtained by the analysis of the signals into classes, which correspond to the different modes of operation of the machine to be studied, by a similarity measure such as the hierarchical methods. The DC voltage fault in SRM is presented in [10], a new method of detection based on K-Means clustering technique is introduced. However, these methods require an initial partition with a defined number of classes. These constraints are a disadvantage when the learning base is not entirely determined. An artificial neural network based fault identification method for H-Bridge converter associated with SRM is presented in [11]. The proposed fault diagnostic system identifies the fault with accuracy, but it takes enormous training time (7000 neurons have been used as input).
Although open-circuit faults are a common fault type in electric machine drive, the detection of this fault is rarely treated in literature for the SRM drive. That due to the capacity of the machine to continue operating under these faults and the simplicity of its detection by using current sensors. However, in the electric powertrain applications, it is crucial to detect and localize automatically the open-circuit faults which can lead to starting difficulties, overcurrents, high torque ripples and reduced load capacity [12].
In this context, the purpose of this paper is to present an automatic methodology based on the fast Fourier transform (FFT) algorithm with a new sliding periodical window proposed to detect and localize the open-phase faults.

II. SRM MODELLING

Despite the simplicity of its construction, the mathematical model of the machine is relatively complicated because of its dominant nonlinear behavior. The flux-linkages is a function of two variables; the rotor position and the stator current.

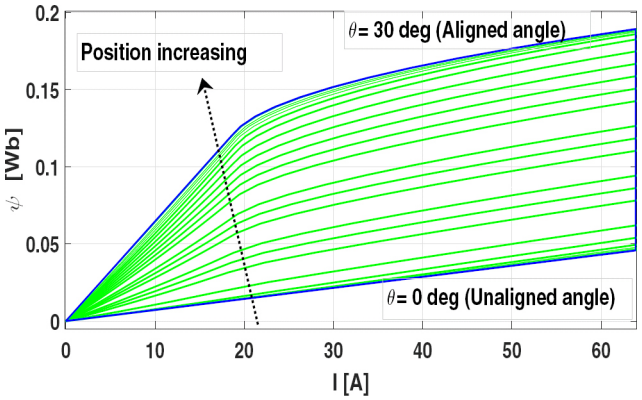

Fig. 1: Flux-linkage of the SRM.

Nomenclature:

θ	Rotor position	I_j	Current in the j^{th} phase
Ω	Angular velocity of rotor	ψ_j	Flux-linkages in j^{th} phase
T_e	Total electromagnetic torque	R_j	Resistance of the j^{th} phase
f_r	Friction coefficient	L	Instantaneous inductance
J	Total inertia (rotor and load)	V_j	Voltages of the j^{th} phase
J_{load}	Vehicle inertia	J_{SRM}	Machine inertia
T_L	Load torque		

In this study, the SRM used has 4 phases of $8/6$-type. The flux-linkages of one phase is presented in Fig. 1 where its parameters are given in the appendix. The mathematical model of the equivalent electrical circuit is given by [3]:

$$V_j = R_j I_j + \frac{\partial \psi_j(\theta, I)}{\partial t} \tag{1}$$

with $j = 1, 2, 3, 4$.
The mecanical model of the SRM associated to a load can be expressed as:

$$\begin{cases} \frac{\mathrm{d}\Omega}{\mathrm{dt}} = \frac{1}{J}\left(T_e(\theta, I) - f_r\Omega - T_L\right) \\ J = J_{load} + J_{SRM} \end{cases} \tag{2}$$

And the instantaneous torque developed by the phase j is [3]:

$$T_{phase_j} = \frac{1}{2}\frac{\mathrm{dL}(\theta)}{\mathrm{d}\theta} I_j^2 \tag{3}$$

The equation (3) is applied only in the case of magnetic linearity. In this research, the T_{phase_j} is calculated using the torque-linkage which is a nonlinear function of the stator phase current and rotor position [5].
The instantaneous torque developed by the machine is the sum of the instantaneous torques developed by each phase:

$$T_e = \sum_{j=1}^{j=4} T_{phase_j} \tag{4}$$

III. TIME-PLAN ANALYSIS OF SRM OPEN-CIRCUIT FAULT

In this part based on the vehicle drivetrain, a frequency analysis behavior is carried out in healthy and faulty modes for different temporal responses. For faulty mode, an open-circuit is created in the converter associated to the SRM.

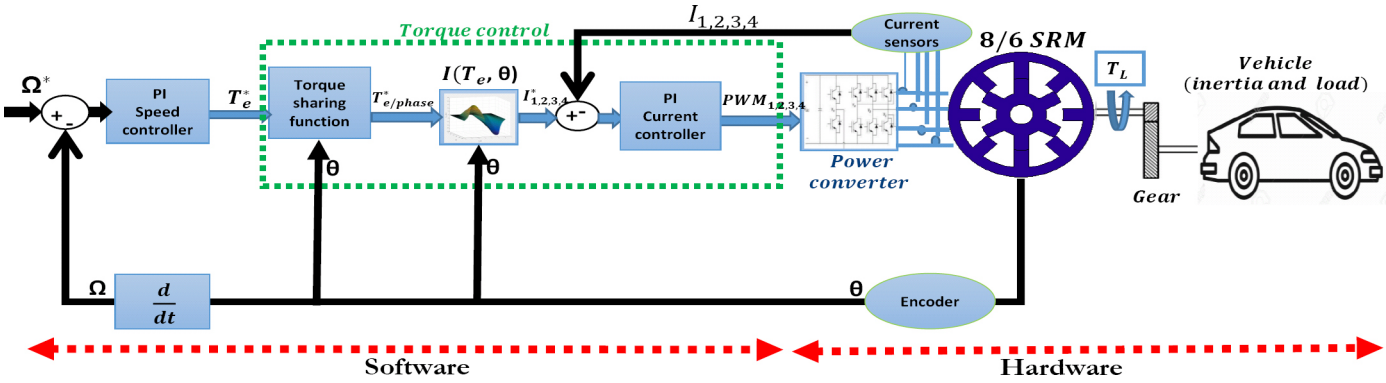

Fig. 2: Cascade control strategy of the SRM in the electric vehicle drivetrain.

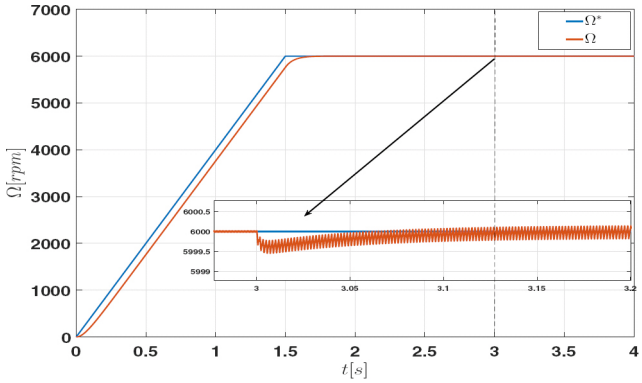

Fig. 3: Velocity response of the SRM.

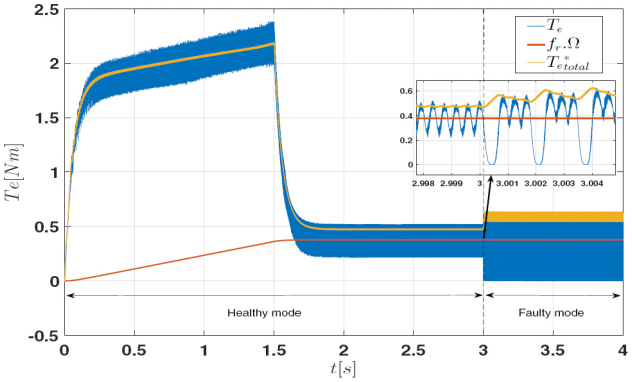

Fig. 4: Torque responses of the SRM.

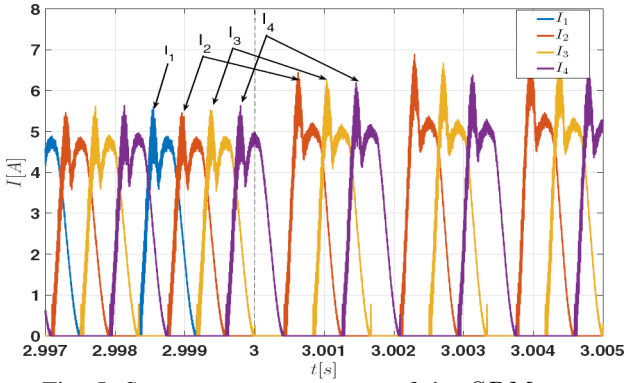

Fig. 5: Stator current responses of the SRM.

A. Drivetrain description

The vehicle powertrain shown in Fig.2 is mainly composed of SRM associated, by a gear, to a vehicle load and supplied by a power converter/battery. For the control, a cascade control scheme approach is adopted in this study using velocity and current controllers. Also, position and current sensors are associated respectively to the control loops designed using PI controllers. The external control loop (velocity loop) provides the total reference torque (T_e^*) to the torque sharing function which is in charge to give the reference torque of each phase ($T^*_{e/phase}$). Using the characteristics $I(Te, \theta)$, the reference currents are finally deduced for the internal control loops (current loops).

B. Open-circuit fault simulation

To simulate the open-circuit fault in the machine winding, an ideal switch is used to make the connection between the inverter arm and the phase A of the machine with no load torque. When the steady-state velocity is reached the switch is opened (at $t = 3s$).
Fig.3 shows the effect of the open-circuit fault on the velocity response at steady state. Indeed, it does not affect the stability of machine operation, but a small velocity drop has occurred at the instant of the fault creation. Also, after reaching the same steady-state value, a weak fluctuation has appeared. This is due to the loss of the torque in phase A and its compensation by the other phases as shown in figure Fig.4. However, the machine torque is reduced to three-quarters of the total torque in healthy mode while the average torque in steady-state is equal to the viscous friction torque ($f_r\Omega$). Nevertheless, this induces a significant torque ripple because of losing the A phase current (Fig.5).

IV. Frequency analysis of SRM open-circuit fault

As shown previously, the loss of a machine phase causes a change in the amplitude of the stator currents and the total reference torque responses. In order to detect and locate the open circuit fault of the machine phases, a frequency analysis method is proposed. In this method, a spectral analysis of currents and total reference torque signals is carried out using Fast Fourier Transform (FFT) algorithm with a new approach of sliding periodic window.

A. Proposed sliding periodic window

To analyze the frequency spectrum of the desired signals (stator currents and total torque reference), we propose to apply the FFT on a small sliding time interval including a full period of the signal. The choice of this interval is based on the fundamental frequencies of the phase current [3] :

$$f_1 = \frac{n}{60} N_r \tag{5}$$

Where n is the machine velocity in r.p.m and N_r is the number of the rotor poles.
To take into account, the time-plane offset between two successive signals of the four currents at the instant t, the step angle (offset) is defined by [3]:

$$\xi = \frac{2\pi}{mN_r} \tag{6}$$

Where m is the machine phases number.
To use simultaneously, for the four currents, the same sliding window at the same instant, the window width (W_{width}) must include two periods of each signal:

$$W_{width} = \frac{2}{f_1} \tag{7}$$

B. Frequency spectrum analysis

Using the proposed sliding periodic window, the FFT algorithm is therefore applied to the selected signals (currents and total reference torque). A comparison is carried out on the amplitude of the fundamental fraquency (f_1) of each signal spectrum in healthy and faulty modes.

1) Frequency spectrum analysis of currents: the FFT is applied simultaneously for the four currents inside the proposed sliding periodic window. In the beginning, an open-circuit is created in phase A at $t = 3s$ where the SRM, without load torque, is at its steady-state velocity of 6000 rpm. Fig. 5 illustrates the current responses of all the phases where the current of phase A is null from the instant of fault creation. Also, the other currents of the remaining phases are undergone successively amplitudes change. Indeed, the current amplitude of the flowing phase which is B is more significant compared to the others. In Fig. 6, an illustration of the proposed approach is presented using the current of phase B. Fig. 6a shows the selected sliding periodic window in the time domain. Based on the FFT algorithm inside this window, a frequency analysis is done (Fig. 6b) in order to quantify the amplitude change in the fundamental frequency ($f_1 = 600Hz$) which is more significant compared to the harmonics amplitude.
Table. I summarizes the current spectrum amplitude change at the fundamental frequency (f_1) creating separately the open-circuit fault in each phase at $\Omega^* = 6000$ rpm and $T_L = 0$ Nm.

Phase current	Current spectrum amplitudes at f_1				
	Healthy mode	Phase A open	Phase B open	Phase C open	Phase D open
I_1	2.4	0	2.7	2.8	2.9
I_2	2.4	2.9	0	2.7	2.8
I_3	2.4	2.8	2.9	0	2.7
I_4	2.4	2.7	2.8	2.9	0

TABLE I: Current amplitudes in healthy and faulty modes.

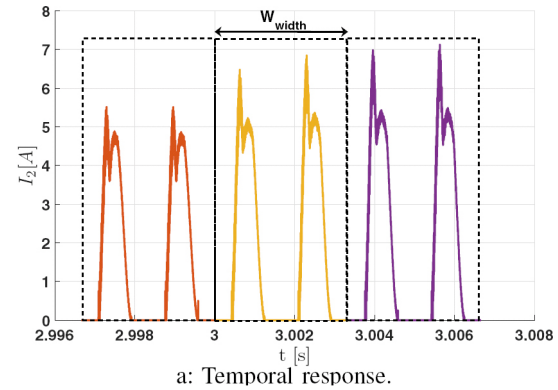

a: Temporal response.

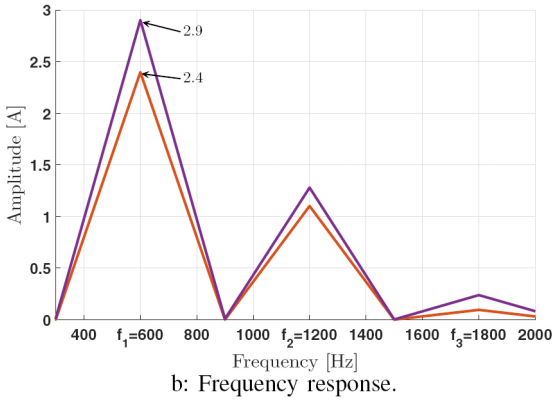

b: Frequency response.

Fig. 6: Current responses of phase B.

Based on the results of Table 1, we noticed that the open-circuit fault created the same behavior in each phase. However, if a phase is disconnected, its amplitude at f_1 is null while the amplitude of the following phases are increased respectively from $2.4A$ in healthy mode to $2.9A$, $2.8A$ and $2.7A$.
In the proposed approach, the spectrum amplitude change at the fundamental frequency (ΔA_{f_1}) of each current is quantified in percentage between healthy and faulty modes:

$$\Delta A_{f_1}(\%) = \frac{A_{hm\,f_1} - A_{fm\,f_1}}{A_{hm\,f_1}} \times 100 \tag{8}$$

$A_{hm\,f_1}$ and $A_{fm\,f_1}$ are respectively the spectrum amplitude at the fundamental frequency in healthy and faulty modes.
Using (8), a quantification of the spectrum amplitude change of the current phases in % is computed between of healthy and faulty modes of phase A: $\Delta I_{2\,f_1} = 20.83\%$, $\Delta I_{3\,f_1} = 16.66\%$ and $\Delta I_{4\,f_1} = 12.5\%$.
To obtain a general mapping, this study is extended taking into account the velocity and the load torque variations. First, the influence of velocity change with zero load torque is simulated and the obtained results are presented in Table. IIa. Secondly, the impact of load torque at a constant velocity is simulated too. The obtained results are given in Table. IIb. Finally, a simulation is effected combining the change of the velocity and the load torque. The results of this simualtion are summarized in Table. IIc.
The obtained results show that the spectrum amplitude changes at the fundamental frequency of the currents are not almost

affected by the variations of the velocity and the load torque. Moreover, this change can be an indicator to locate the open-circuit fault which can occur in any phase. If a phase is disconnected, its spectrum amplitude at f_1 is zero and the amplitude of the neighboring phase is increased by about 20% whatever the velocity and the load torque maybe.

2) Frequency spectrum analysis of the total reference torque: using the same approach with the same sliding periodic window in healthy and faulty modes, an analysis of the spectrum amplitude change for the total reference torque (T_e^*) at the fundamental frequency is done.
Fig.7 illustrates the total reference torque response for $\Omega = 6000$ rpm and $T_L = 0$ Nm.
Where a general mapping of the spectrum amplitude change, at the fundamental frequency (f_1), for different values of velocity and load torque are summarized in Table.III.

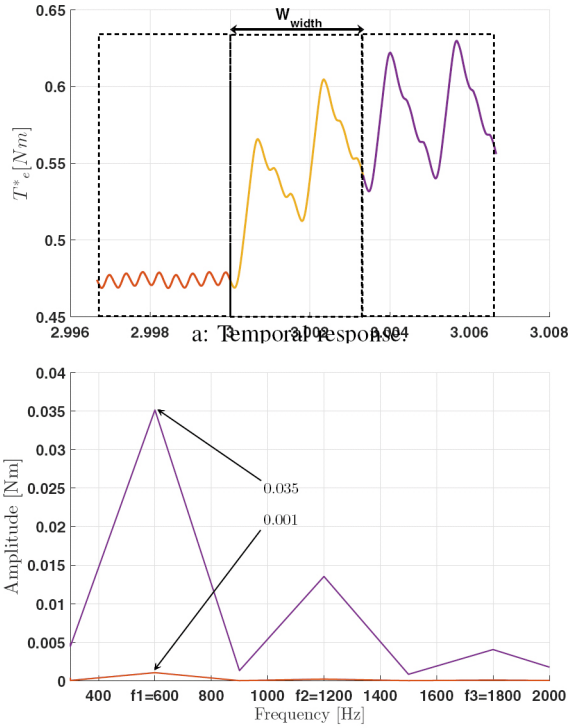

a: Temporal response.

b: Frequency response.

Fig. 7: Total reference torque response.

The results obtained prove that the amplitude variations at the fundamental frequency of the total reference torque can be an indicator to detect the open circuit fault of any phase. If a phase is disconnected, the amplitude of the T_e^* at f_1 varise between 3000% and 3400%.

V. Fault Detection and Localization Method Based on Spectrum Analysis

Based on the frequency analysis of the four currents and the total reference torque, a methodology to detect and to locate automatically the open-circuit fault in any phase is proposed.

velocity [rpm]	Currents spectrum amplitudes at f_1 [A]			
	Current	Healthy	Faulty	Increase [%]
2000	I_1	1.36	0	/
	I_2	1.36	1.62	19.13
	I_3	1.36	1.57	16.01
	I_4	1.36	1.51	11.21
4000	I_1	1.93	0	/
	I_2	1.93	2.30	19.58
	I_3	1.93	2.25	16.74
	I_4	1.93	2.14	11.36
6000	I_1	2.4	0	/
	I_2	2.4	2.9	20.83
	I_3	2.4	2.8	16.66
	I_4	2.4	2.7	12.50
8000	I_1	2.8	0	/
	I_2	2.8	3.37	20.66
	I_3	2.8	3.27	17.01
	I_4	2.8	3.13	12.13
10000	I_1	3.14	0	/
	I_2	3.14	3,74	19,10
	I_3	3.14	3,71	18,15
	I_4	3.14	3,63	15,60

a: Current amplitude quantifications in terms of velocity.

T_L [Nm]	Currents spectrum amplitudes at f_1 [A]			
	Current	Healthy	Faulty	Increase [%]
0	I_1	2.4	0	/
	I_2	2.4	2.9	20.83
	I_3	2.4	2.8	16.66
	I_4	2.4	2.7	12.50
2	I_1	6.62	0	/
	I_2	6.62	7.93	19.78
	I_3	6.62	7.76	17.22
	I_4	6.62	7.47	12.83
4	I_1	9.25	0	/
	I_2	9.25	11.19	20.97
	I_3	9.25	10.83	17.08
	I_4	9.25	10.44	12.91
6	I_1	11.52	0	/
	I_2	11.52	14.15	22.82
	I_3	11.52	13.68	18.75
	I_4	11.52	13.01	13.02
8	I_1	13.72	0	/
	I_2	13.72	16.68	21.63
	I_3	13.72	16.31	18.93
	I_4	13.72	15.51	13.06

b: Current amplitude quantifications in terms of load torque.

Ω^* [rpm]	T_L[Nm]	Currents spectrum amplitudes at f_1 [A]			
		Current	Healthy	Faulty	Increase %
2000	0	I_1	1.36	0	/
		I_2	1.36	1.62	19.13
		I_3	1.36	1.57	16.01
		I_4	1.36	1.51	11.21
4000	2	I_1	6.43	0	/
		I_2	6.43	7.84	21.92
		I_3	6.43	7.61	18.35
		I_4	6.43	7.25	12.75
6000	4	I_1	9.25	0	/
		I_2	9.25	11.28	20.94
		I_3	9.25	10.97	18.59
		I_4	9.25	10.63	14.91
8000	6	I_1	11.63	0	/
		I_2	11.63	14.00	20.37
		I_3	11.63	13.67	17.54
		I_4	11.63	13.33	14.61
10000	8	I_1	13.45	0	/
		I_2	13.45	16.44	22.23
		I_3	13.45	15.78	18.01
		I_4	13.45	15.06	12.03

c: Current amplitude quantifications in terms of velocity and load torque.

TABLE II: Summary of current amplitude quantifications.

Ω^* [rpm]	T_L [Nm]	T_e^* spectrum amplitudes at f_1 [Nm]			
			Healthy	Faulty	Increase %
2000	0	T_e^*	0.001	0.035	3400
4000	2	T_e^*	0.0011	0.0391	3450
6000	4	T_e^*	0.002	0.0698	3390
8000	6	T_e^*	0.0052	0.1908	3570
10000	8	T_e^*	0.018	0.573	3083

TABLE III: Summary total reference torque quantifications.

The flowchart in Fig. 8, summarizes the implementation of the proposed methodology. While the vehicle is running, the current and the total reference torque are measured instantly. The FFT has applied to these signals inside the sliding window at instant t and $t + W_{width}$ at the same time in order to calculate the $\Delta A_{f_1}(\%)$ of each signal. After the quantification of the spectrum amplitude, the open-phase fault is detected when $\Delta T^*_{e\,f_1}(\%) \in [3000, 3500]$. Moreover, the disconnected phase j is located using $\Delta I_{j\,f_1}(\%)$. If its spectrum amplitude quantification is -100% and that of its neighboring phase is about 20%.

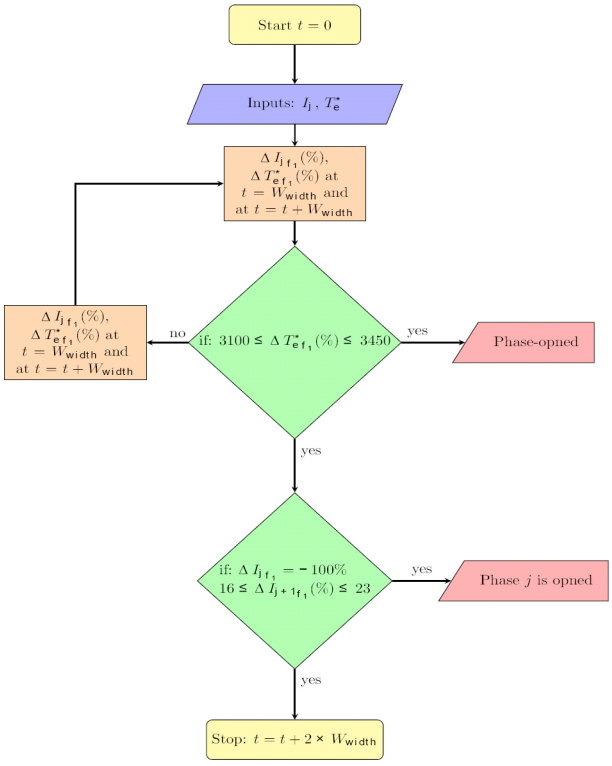

Fig. 8: Proposed strategy implementation.

VI. CONCLUSION

In this paper, automatic detection and localization methodology for an open-circuit fault in any phase of SRM used in electric vehicles application is developed and validated by simulation. This methodology could be useful to be implemented in the control unit of the electric vehicles. However, if any phase is disconnected during driving, the control unit can detect and locate the fault instantaneously to switch to the fault tolerant control if it is implemented in the same control unit or to anticipate the maintenance and consequently its cost.

In this study, the principle of the methodology with a brief description is given. In the future works, the developed approach will take into account more velocity and load torque changes in order to be implemented in the test bench of the electric vehicle emulator with the SRM used for this study. Also, the proposed methodology will be extended to detect and locate more than one open-phase fault.

APPENDIX

Parameter	**Value**
Topology	8S/6R
Phase number	4
Power supply (DC)	250 V
Maximum current	61 A
Nominal torque	20 Nm
Nominal Power	8 kW
Maximum speed	10000 rpm
Phase resistance R	0.0404 Ohm
Moment of inertia J_{SRM}	0.0043 Kg/m2
Friction f_r	0.005 Nm/s

REFERENCES

[1] J. D.Widmer, R. Martin, M. Kimiabeigi, "Electric vehicle traction motors without rare earth magnets," Sustainable Materials and Technologies, vol. 3, pp. 7-13, April 2015.

[2] Kamalakannan, C., et al. "Switched reluctance machine in automotive applications—A technology status review." Electrical Energy Systems (ICEES), 2011 1st International Conference on. IEEE, 2011.

[3] Krishnan, Ramu. Switched reluctance motor drives: modeling, simulation, analysis, design, and applications. CRC press, 2001.

[4] M. Takiguchi, H. Sugimoto, N. Kurihara and A. Chiba, "Acoustic Noise and Vibration Reduction of SRM by Elimination of Third Harmonic Component in Sum of Radial Forces," in IEEE Transactions on Energy Conversion, vol. 30, no. 3, pp. 883-891, Sept. 2015.

[5] Y. Saadi, R. Sehab, A. Chaibet, M. Boukhnifer and D. Diallo, "Performance Comparison between Conventional and Robust Control for the Powertrain of an Electric Vehicle Propelled by a Switched Reluctance Machine," 2017 IEEE Vehicle Power and Propulsion Conference (VPPC), Belfort, 2017, pp. 1-6.

[6] Y. Saadi, R. Sehab, A. Chaibet, M. Boukhnifer and D. Diallo, "Sensorless control of switched reluctance motor for EV application using a sliding mode observer with unknown inputs," 2018 IEEE International Conference on Industrial Technology (ICIT), Lyon, 2018, pp. 516-521.

[7] S. Gopalakrishnan, A. M. Omekanda and B. Lequesne, "Classification and remediation of electrical faults in the switched reluctance drive," in IEEE Transactions on Industry Applications, vol. 42, no. 2, pp. 479-486, March-April 2006.

[8] C. M. Stephens, "Fault detection and management system for fault-tolerant switched reluctance motor drives," in IEEE Transactions on Industry Applications, vol. 27, no. 6, pp. 1098-1102, Nov.-Dec. 1991.

[9] Belfore, Lee A., and A. Arkadan. "A methodology for characterizing fault tolerant switched reluctance motors using neurogenetically derived models." IEEE Transactions on Energy Conversion 17.3 (2002): 380-384.

[10] Chandrika, V., and A. Ebenezer Jeyakumar. "Detection of DC voltage fault in SRM drives using k-means clustering and classification with SVM." Int. J. Mod. Eng. Res.(IJMER) 1.4 (2014): 38-42.

[11] Salankayana, S. K., N. Chellammal, and Ravitheja Gurram. "Diagnosis of faults due to misfiring of switches of a cascaded h-bridge multilevel inverter using artificial neural networks." International Journal of Computer Applications 41.17 (2012).

[12] D. Diallo, M. E. H. Benbouzid and A. Makouf, "A fault-tolerant control architecture for induction motor drives in automotive applications," in IEEE Transactions on Vehicular Technology, vol. 53, no. 6, pp. 1847-1855, Nov. 2004.